

New fitting scheme to obtain effective potential from Car-Parrinello molecular dynamics simulations : Application to silica

A. CARRÉ^{1,2}, J. HORBACH^{1,3}, S. ISPAS² and W. KOB²

¹ *Institut für Physik, Johannes Gutenberg-Universität Mainz, Staudinger Weg 7, 55099 Mainz, Germany*

² *Laboratoire des Colloïdes, Verres et Nanomatériaux, Université Montpellier II and CNRS UMR 5587, 34095 Montpellier, France*

³ *Institut für Materialphysik im Weltraum, Deutsches Zentrum für Luft- und Raumfahrt (DLR), 51170 Köln, Germany*

PACS 71.15.Pd – Molecular dynamics calculations (Car-Parrinello) and other numerical simulations

PACS 71.15.Mb – Density functional theory, local density approximation, gradient and other corrections

PACS 61.43.Fs – Glasses

PACS 61.20.Ja – Computer simulation of liquid structure

Abstract. - A fitting scheme is proposed to obtain effective potentials from Car-Parrinello molecular dynamics (CPMD) simulations. It is used to parameterize a new pair potential for silica. MD simulations with this new potential are done to determine structural and dynamic properties and to compare these properties to those obtained from CPMD and a MD simulation using the so-called BKS potential. The new potential reproduces accurately the liquid structure generated by the CPMD trajectories, the experimental activation energies for the self-diffusion constants and the experimental density of amorphous silica. Also lattice parameters and elastic constants of α -quartz are well-reproduced, showing the transferability of the new potential.

Introduction. – One of the central issues of atomistic computer simulations is to develop effective potentials [1] that model the interactions between ions by some functional form without taking into account explicitly the electronic degrees of freedom. The first step to obtain such a potential for a given system is to decide its functional form. In terms of computational efficiency, an optimal ansatz is provided by a pair potential model. However, for a realistic modelling it might be often necessary to include many-body terms to describe, e.g., three-body interactions or polarizability effects. In a second step, the free parameters of the potential function have to be fitted to experimental data and/or to *ab initio* calculations [2,3]. A relatively new approach is to use *ab initio* molecular dynamics simulations such as Car-Parrinello molecular dynamics (CPMD) [4] for the parametrization of effective potentials. The latter simulation technique has been proven very successful to realistically describe a large number of atomistic systems, among them network forming systems such as silica [5–10]. Nowadays, systems of 100 to 200 particles can be simulated on a time scale of several tens

of picoseconds by CPMD.

In this Letter, we aim at developing a fitting scheme for the parametrization of effective potentials from CPMD trajectories and we address this issue to the case of liquid silica. A widely-used method for the parametrization of potentials is the so-called force matching procedure [11] where one tries to match the CPMD forces on the atoms with those resulting from the classical potential. However, we have found that, in the case of silica, the force matching method fails (at least if a pair potential model is considered) [12]: Although the CPMD forces are well reproduced by the resulting effective (pair) potential, the structure is very different from that obtained by CPMD. The main aim of this work is to develop a different fitting scheme where one tries to match as closely as possible the atomistic structure, as obtained from the classical MD using the effective potential, with that of the CPMD.

Since silica is of great importance for technological applications, geosciences and the theory of the glass transition, the development of effective potentials for silica has a long history [2,3,13–18]. Surprisingly, various stud-

ies have shown that a simple pair potential, the so-called BKS potential [2], is able to give a quite accurate description of amorphous silica [8, 19–22]. The parametrization of this potential was based on Hartree-Fock calculations of a single SiO_4 tetrahedron (saturated by four hydrogen atoms), considering also experimental elastic constants of α -quartz in the fitting procedure.

Unsurprisingly, the BKS model has also several deficiencies. For instance, the equation of state, as far as it is known experimentally, is not reproduced well [3]. One could argue that one has to include many body effects to overcome the deficiencies of the BKS potential. However, as shown in Ref. [22], more complicated potentials that include polarizability effects or fluctuating charges do not provide necessarily a more realistic description of silica.

Here, we demonstrate that one can improve the accuracy of a pair potential for amorphous silica. The idea of our approach is to match the partial pair correlation functions, as obtained from the effective potential, with those obtained from a CPMD simulation. As demonstrated below, the new potential yields an accurate description of amorphous silica with respect to density, structure and diffusion dynamics. Also properties of α -quartz are well reproduced by the new potential. The fitting scheme proposed in this work can be also used for other systems and it is not restricted to the parametrization of pair potentials.

Simulation details and fitting methodology. –

Ab initio simulations. CPMD simulations [23] were done for a system of 38 SiO_2 units (114 atoms) in a cubic box of size $L = 11.982 \text{ \AA}$, corresponding to the experimental density of 2.2 g/cm^3 [24]. Periodic boundary conditions are used in all three spatial directions. The electronic structure was described by the local density approximation (LDA) in the framework of density functional theory [25]. Norm-conserving pseudopotentials were used for silicon [26] and oxygen [27], and the plane-wave basis sets were expanded up to an energy cut-off of 70 Ry. The choice of pseudopotentials, exchange and correlation functionals and the plane-wave cutoff are justified by previous CPMD studies carried out on amorphous SiO_2 [8–10].

A time step of 3 a.u. (0.0725 fs) and a fictitious electronic mass of 600 a.u. were used to integrate the equations of motion. Temperature is kept constant by applying Nosé-Hoover chains for each ionic degree of freedom [28, 29] as well as for the electronic degrees of freedom to counterbalance the energy flow from ions to electrons [30]. The parameters used for the Nosé-Hoover chains can be found in previous publications [8, 9].

The starting configuration for the CPMD was generated by MD simulations with the BKS potential [2], following the same methodology as in Refs. [8, 9]. Then, a CPMD run over about 20 ps at $T = 3600 \text{ K}$ was performed from which we used the last 16.5 ps for the analysis.

Fitting procedure. The next step was to obtain an effective potential from the CPMD data. To this end, we aimed at parameterizing a given potential model such that

the partial pair correlation functions $g_{\alpha\beta}(r)$ ($\alpha\beta \in \{\text{Si}, \text{O}\}$) [31], as calculated from the CPMD trajectories, were reproduced by the MD simulations using the new potential.

As an ansatz for the effective potential we used the same functional form as the one used for the BKS potential,

$$u_{\alpha\beta}(r) = \frac{q_\alpha q_\beta e^2}{r} + A_{\alpha\beta} \exp(-B_{\alpha\beta} r) - \frac{C_{\alpha\beta}}{r^6}, \quad (1)$$

where r is the distance between an ion of type α and an ion of type β ($\alpha, \beta = \text{Si}, \text{O}$) and e is the elementary charge. We consider the parameters appearing in Eq. (1) as elements of the vector $\xi = (\xi_k, k = 1, 2, \dots, 10) = (q_{\text{Si}}, A_{\alpha\beta}, B_{\alpha\beta}, C_{\alpha\beta}, \alpha, \beta \in \{\text{Si}, \text{O}\})$. The effective charge for the oxygen atoms does not appear in the ξ vector since, due to the charge neutrality requirement, it is directly related to the silicon charge via $q_{\text{O}} = -q_{\text{Si}}/2$. Forces and energies that correspond to the long-ranged Coulomb terms in (1) have been computed by Ewald sums [32], those for the short-range part in (1) have been truncated and shifted at 6.5 \AA . In addition a smoothening function was used for the short-range part to avoid a drift of the total energy in microcanonical MD runs. The details of this function can be found in a recent MD study with the BKS model [33].

The cost function χ^2 that measures the difference between the CPMD data and the fitting model is based on the pair correlation functions weighted by the distance r , $rg_{\alpha\beta}(r)$,

$$\chi^2 = \int_0^{L/2} \lambda^2(r) dr, \quad (2)$$

where $\lambda^2(r)$ is defined as follows:

$$\lambda^2(r) = \sum_{\alpha, \beta = \text{Si}, \text{O}} [rg_{\alpha\beta}^{\text{CPMD}}(r) - rg_{\alpha\beta}^{\text{CHIK}}(r; \xi)]^2. \quad (3)$$

Here, the superscripts CPMD and CHIK indicate respectively the use of CPMD and MD with the new potential, that we call CHIK potential in the following. The integral (2) was evaluated by numerical integration. Note that a cost function χ^2 in which the function $rg_{\alpha\beta}(r)$ in Eq. (3) is replaced by $g_{\alpha\beta}(r)$ or $r^2 g_{\alpha\beta}(r)$ resulted in potentials that were not accurate [12]. The reason for this is that $rg_{\alpha\beta}(r)$ makes a good compromise between weighting the structural information at short distances, such as is done by the cost function with $g_{\alpha\beta}(r)$, and long distances, as is done by the cost function with $r^2 g_{\alpha\beta}(r)$.

The optimal vector ξ of the potential parameters was determined by an iterative Levenberg-Marquardt algorithm [34]. After each iteration step, ξ was updated leading to a new guess for the potential. This potential was then used in MD simulations yielding a new set of pair correlation functions $g_{\alpha\beta}^{\text{CHIK}}(r; \xi)$. Recall that the Levenberg-Marquardt algorithm requires the calculation of the derivatives of the $g_{\alpha\beta}$ with respect to the potential parameters. These derivatives were computed numerically by finite differences:

$$\frac{\partial g_{\alpha\beta}(r, \xi)}{\partial \xi_k} = \lim_{\varepsilon_k \rightarrow 0} \frac{g_{\alpha\beta}(r, \xi_k + \varepsilon_k) - g_{\alpha\beta}(r, \xi_k - \varepsilon_k)}{2\varepsilon_k}. \quad (4)$$

Parameter	CHIK
q_{Si} (C)	1.910418
A_{OO} (eV)	659.595398
B_{OO} (\AA^{-1})	2.590066
C_{OO} (eV. \AA^6)	26.836679
A_{SiO} (eV)	27029.419922
B_{SiO} (\AA^{-1})	5.158606
C_{SiO} (eV. \AA^6)	148.099091
A_{SiSi} (eV)	3150.462646
B_{SiSi} (\AA^{-1})	2.851451
C_{SiSi} (eV. \AA^6)	626.751953

Table 1: Parameters of the CHIK potential.

Here, small perturbations ($\pm \varepsilon_k$) of a given parameter ξ_k are considered, keeping all other parameters constant.

MD simulations were performed to compute the functions $g_{\alpha\beta}^{\text{CHIK}}(r; \xi)$ and the derivatives (4). In these simulations, we considered a system of 1152 atoms in a cubic box of size 25.9\AA (corresponding to the density $\rho = 2.2 \text{ g/cm}^3$). The simulations were done in the *NVT* ensemble at the temperature $T = 3600 \text{ K}$. Temperature was kept constant by coupling the system periodically to a stochastic heat bath. The equations of motion were integrated by the velocity form of the Verlet algorithm, using a time step of 1.0 fs . For an accurate calculation of the functions $g_{\alpha\beta}^{\text{CHIK}}(r; \xi)$, runs over 10 ps were required.

Following the methodology described above, convergence was obtained after 44 iterations yielding the potential parameters¹ that are listed in Tab. 1. We note that these parameters are of the same order of magnitude as the parameters of the BKS potential [2]. Thus, our model can be seen as a modification of the BKS potential which yields already a good description of (amorphous) silica.

MD simulations with the CHIK potential. As a third step extensive MD simulations were performed with the CHIK potential to investigate the temperature dependence of structural and dynamic properties of the new model. We used systems of 1152 particles in a cubic box of size $L = 25.9 \text{\AA}$ corresponding to the density $\rho = 2.2 \text{ g/cm}^3$. Equilibration runs were done at constant temperature (see above), using now a time step of 1.6 fs . After the equilibration, microcanonical production runs were done at the temperatures 5200 K , 4300 K , 4000 K , 3580 K , 3250 K , 3000 K , 2900 K , 2750 K , 2580 K , and 2440 K . At $T = 2440 \text{ K}$, each the equilibration and production runs lasted over 32 million time step corresponding to a real time of 52.3 ns . At each temperature,

¹As the Born-Mayer ansatz diverges for very short distances, the following repulsive interaction has been added to the potential ansatz (1):

$$u_{\alpha\beta}^{\text{cor}}(r) = \frac{D_{\alpha\beta}}{r^{24}}$$

with $D_{\text{OO}} = 113.0 \text{ eV} \cdot \text{\AA}^{24}$, $D_{\text{SiO}} = 29.0 \text{ eV} \cdot \text{\AA}^{24}$, $D_{\text{SiSi}} = 3423200.0 \text{ eV} \cdot \text{\AA}^{24}$.

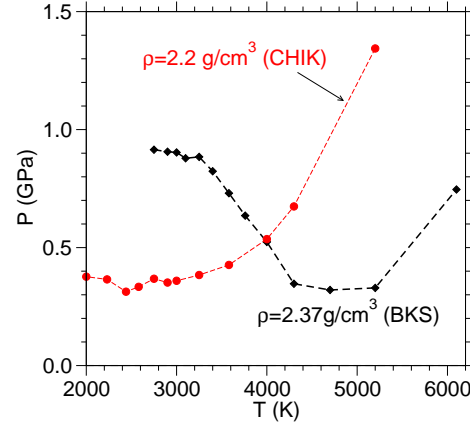


Fig. 1: Temperature dependence of the pressure for the BKS model (from Ref. [20]) and the CHIK model, as indicated.

results were averaged over 8 independent runs. In order to estimate the pressure, additional runs were done at 2230 K and 2000 K . Here, the system was annealed for 15 million time steps. Then the pressure was measured in subsequent runs over 5 million time steps.

For comparison, also results from a previous MD simulation with the BKS model are shown in the following. The details of this simulation can be found in Ref. [20].

Results. –

Static properties. One of the peculiar properties of amorphous SiO_2 is the occurrence of a density maximum at 1820 K [35]. Moreover, in a broad temperature range from room temperature to temperatures above 2000 K the variations of the density around an average value of about 2.2 g/cm^3 are smaller than 1% [24]. These features can also be seen in the temperature dependence of the pressure since the pressure shows a local minimum at the temperature where the density maximum occurs. Both the BKS and the CHIK model show indeed a minimum pressure at about 4800 K and 2300 K , respectively, see Fig. 1. However, the result for the CHIK model is in better agreement with experiment with respect to the location of the minimum and the density. As can be inferred from Fig. 1, at $\rho = 2.2 \text{ g/cm}^3$, a minimum value of about 0.35 GPa is found for the CHIK model. In contrast to this the BKS model has, at a density of $\rho = 2.2 \text{ g/cm}^3$, negative values for the pressure if $T < 7000 \text{ K}$ [19].

Figure 2 shows the partial pair correlation functions at $T = 3600 \text{ K}$, as calculated from CPMD and classical MD using the BKS and the CHIK model. The CHIK model yields good agreement with the CPMD results. The largest differences are found in $g_{\text{SiSi}}(r)$, but also in this case, the CHIK potential leads to a better agreement with CPMD than the BKS potential (see the inset in Fig. 2).

The partial pair correlation functions as obtained from the CPMD run were used to parametrize the CHIK potential. That these functions are reproduced well by the CHIK potential is thus not that surprising. A less ob-

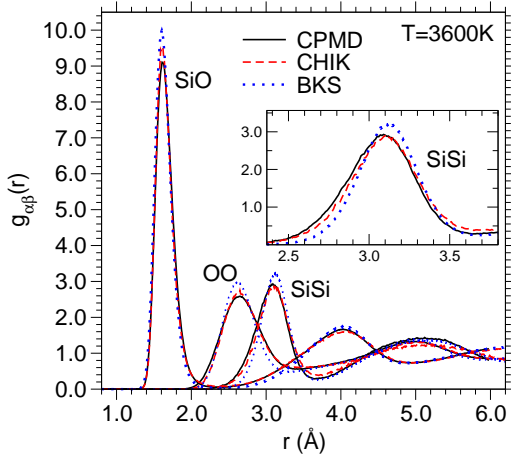


Fig. 2: Partial pair correlation functions at $T = 3600$ K, calculated from CPMD and classical MD using the BKS and the CHIK potentials, as indicated. The inset shows an enlargement of the first peak in $g_{\text{SiSi}}(r)$.

vious test of the CHIK model is provided by considering the distribution functions $P_{\alpha\beta\gamma}$ of the bond angles ($\alpha\beta\gamma = \text{OSiO}, \text{SiOSi}$) in comparison to CPMD. As can be inferred from Fig. 3, the average intra-tetrahedral OSiO angle is around $\theta = 106^\circ$ at 3600 K, both for CPMD and classical MD. However, in the case of the BKS model the function P_{OSiO} is less broad and exhibits a significantly higher amplitude than the CPMD and the CHIK model. Larger differences are seen in the distribution function for the inter-tetrahedral SiOSi angle. While at 3600 K the BKS distribution shows a maximum around $\theta = 147^\circ$, the CHIK potential gives a maximum around $\theta = 141^\circ$, in better agreement with the CPMD value around $\theta = 136^\circ$.

The distribution functions for the SiOSi angle exhibit also a shoulder around $\theta = 90^\circ$ revealing the emergence of edge-sharing tetrahedra at the relatively high temperature $T = 3600$ K [19]. In the BKS case, the latter shoulder has a lower amplitude, indicating a smaller number of edge-sharing tetrahedra. As for P_{OSiO} , the BKS function for P_{SiOSi} is less broad and its main peak has a higher amplitude. In this sense, the BKS model leads to a less disordered structure than the CPMD and the CHIK model. Also included in Fig. 3 is the SiOSi bond angle distribution at 300 K (i.e. in the glass), as obtained from the simulation with the CHIK model (for the preparation of the glass samples, see below the discussion on the calculation of the density of states). In agreement with experimental data [36–38] it shows a shift of the average value for the SiOSi angle from about 140° for the melt at 3600 K to about 150° for the glass structure (note the very good agreement with the value of 151° , obtained by an analysis of NMR data by Mauri *et al* [37]). In contrast to that the BKS potential shows only a slight change of the SiOSi angle from the melt to the glass structure [19].

Dynamic Features. The self-diffusion constants D_α ($\alpha = \text{Si}, \text{O}$) were computed from the long-time limit of

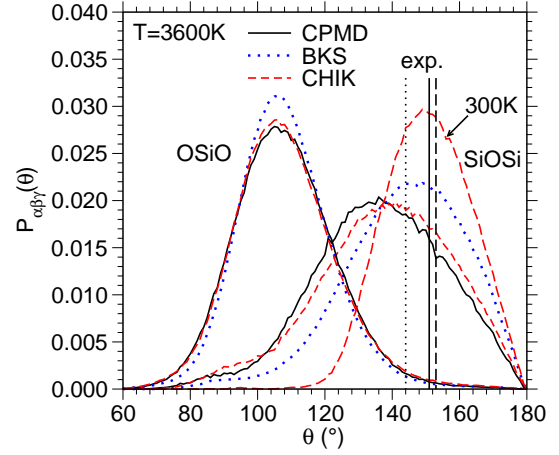


Fig. 3: Angular distribution functions for the OSiO and SiOSi angle at $T = 3600$ K. For the CHIK model, the SiOSi distribution at $T = 300$ K is also included. The vertical lines indicate experimental values from Refs. [36] (dotted line), [37] (solid line), and [38] (dashed line).

the mean squared displacements $\langle r_\alpha^2(t) \rangle$ via the Einstein relation $D_\alpha = \lim_{t \rightarrow \infty} \langle r_\alpha^2(t) \rangle / 6t$ [31, 32]. In Fig. 4, the temperature dependence of the D_α is displayed in an Arrhenius plot. The diffusion dynamics as predicted by the CHIK model appears to be faster than that of the BKS model. At low temperatures ($T \simeq 2750$ K), the self-diffusion coefficients are about a factor of 5 higher than those obtained from the BKS model.

In agreement with various experimental studies [24], at low temperatures the self-diffusion constants can be well-described by an Arrhenius law, $D_\alpha = A_\alpha \exp[-E_a^\alpha / (k_B T)]$. The activation energies E_a , that we find for the CHIK model, are 4.51 eV for oxygen and 4.97 eV for silicon. These values are very similar to those obtained for the BKS model [20] and they are in good agreement with experimental results ($E_a = 4.7$ eV for oxygen [39] and $E_a = 6.0$ eV for silicon [40]).

To compute the vibrational density of states $g(\nu)$ (with ν the frequency), 16 independent and fully equilibrated samples at 2440 K were quenched instantaneously to 300 K, followed by an annealing for 80 ps. Then, $g(\nu)$ was determined by calculating the Fourier transform of the velocity autocorrelation functions for Si and O (for details see Ref. [21]). In Fig. 5, the so-obtained density of states is compared to results from CPMD (from Ref. [10]) and MD simulations using the BKS potential (from Ref. [21]).

A prominent feature in $g(\nu)$ is the double-peak in the frequency band above about 28 THz. The vibrational excitations in this band correspond to stretching modes of the Si-O bond [31]. Note that the BKS potential has been fitted to reproduce the high frequency band of the vibrational spectrum. Thus, it is not surprising that it is in better agreement with CPMD than the CHIK model, since we have not included any vibrational properties in the fitting procedure of the CHIK potential. The CHIK model seems

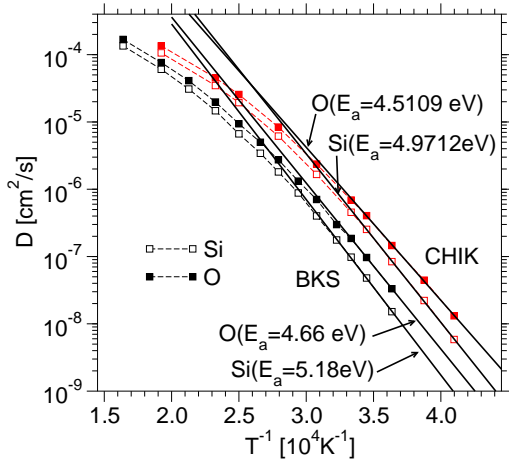


Fig. 4: Arrhenius plot of the self-diffusion constants obtained by simulations with the BKS and the CHIK potentials. The bold solid lines are fits with Arrhenius laws (see text).

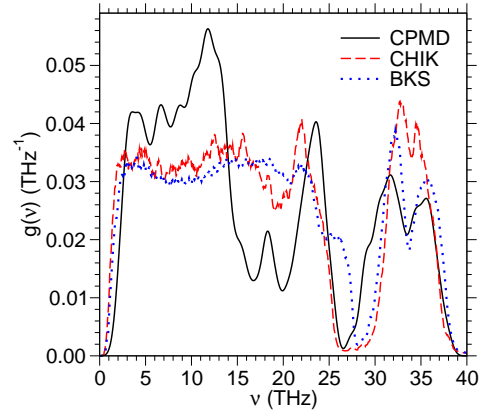


Fig. 5: Density of states from the different MD simulations, as indicated.

to be better than the BKS model in the intermediate frequency band $20 \text{ THz} \leq \nu \leq 30 \text{ THz}$ where, in contrast to the BKS case, a single peak is observed, albeit at a slightly lower frequency than in CPMD result. Below 20 THz the BKS and CHIK results are very similar and do not agree well with the CPMD result. In order to significantly improve the description of the density of states it might be necessary to account for polarization effects in the model potential, as suggested by Wilson *et al.* [16].

α -quartz. We have also carried out calculations on α -quartz to check the transferability of our potential. In the experimental phase diagram [31], α -quartz is the stable phase in the low temperature domain (i.e. up to 846 K). As already mentioned, some of the crystalline properties of α -quartz, i.e. different lattice parameters and elastic constants, have been used for the parametrization of the BKS potential [2]. We have also calculated these quantities using our potential (now using a cutoff at 10 Å for the short-ranged part of the potential). For this, the GULP code [41] was employed which yields the different lattice properties at 0 K. The results are summarized in Tables (2) and (3), in comparison to those predicted by the BKS model and to experimental data (the latter at 300 K!). The CHIK potential reproduces the experimental data with comparable accuracy as the BKS potential, thus indicating that it is also well suited for the study of crystalline SiO_2 phases.

Conclusions. — This work was devoted to the development of a new effective potential for silica. We have presented a fitting scheme for deriving effective potentials from *ab initio* simulations (CPMD). The new potential (named CHIK potential) is superior to the BKS model with respect to various static and dynamic properties of amorphous silica. The CHIK potential is also found to be transferable to other phases such as α -quartz, considering the quantitative agreement between the experimental data for both cell parameters and elastic constants. The fitting

scheme proposed in this study is well-suited to parametrize potentials for other (amorphous) systems, in particular for mixtures of SiO_2 with other oxides such as alkali oxides or Al_2O_3 where the local structure of the melt or the glass can be very different from that of crystalline phases.

* * *

We are grateful to Kurt Binder for very valuable discussions. We thank Schott-Glaswerke Mainz for financial support through the Schott-Glaswerke-Fond and the French Minister of National Education for his administrative funds (co-tutelle). Computing time on the JUMP at the NIC Jülich, on the CINES at Montpellier as well as the IDRIS at Orsay (France) are gratefully acknowledged.

REFERENCES

- [1] FINNIS M., *Interatomic forces in condensed matter* (Oxford University Press, Oxford) 2003
- [2] VAN BEEST B.W.H., KRAMER G.J. and VAN SANTEN R.A., *Phys. Rev. Lett.*, **64** (1990) 1955
- [3] TANGNEY P. and SCANDOLO S., *J. Chem. Phys.*, **117** (2002) 8898
- [4] CAR R. and PARRINELLO M., *Phys. Rev. Lett.*, **55** (1985) 2471
- [5] PASQUARELLO A., SARNTHEIN J. and CAR R., *Phys. Rev. B*, **57** (1998) 14133
- [6] SARNTHEIN J., PASQUARELLO A. and CAR R., *Phys. Rev. Lett.*, **74** (1995) 4682; *Phys. Rev. B*, **52** (1995) 12690.
- [7] UMARI P. and PASQUARELLO A., *Phys. Rev. Lett.*, **98** (2007) 176402
- [8] BENOIT M., ISPAS S., JUND P. and JULLIEN R., *Euro. Phys. J. B*, **13** (2000) 631
- [9] BENOIT M., ISPAS S. and TUCKERMAN M.E., *Phys. Rev. B*, **64** (2001) 224205
- [10] BENOIT M. and KOB W., *Europhys. Lett.*, **60** (2002) 60
- [11] ERCOLESSI F. and ADAMS J.B., *Europhys. Lett.*, **26** (1994) 583
- [12] CARRÉ A., *PhD Thesis* (Universität Mainz, Germany, and Université Montpellier 2, France) 2007

Parameters	Exp. [42]	BKS		CHIK	
		value	error %	value	error %
$V(\text{\AA}^3)$	112.933	115.2	2.0	121.6	7.7
$a(=b)(\text{\AA})$	4.91239	4.940	0.6	5.045	2.7
$c(\text{\AA})$	5.40385	5.448	0.8	5.520	2.1
u	0.4701	0.4648	1.1	0.4732	0.6
x	0.4139	0.4268	3.1	0.4268	3.1
y	0.2674	0.2715	1.5	0.2597	2.8
z	0.2144	0.2085	2.7	0.2012	6.1

Table 2: Lattice parameters for α -quartz for the BKS and the CHIK model, in comparison to experiment.

Elastic Constant (GPa)	Exp. [43, 44]	BKS		CHIK	
		value	error %	value	error %
C_{11}	86.8	90.6	4.2	91.9	5.8
C_{33}	105.8	107.0	1.1	91.6	-13.4
C_{44}	58.2	50.2	-13.7	46.9	-19.4
C_{66}	39.9	41.2	3.2	42.6	6.7
C_{12}	7.0	8.1	15.7	6.6	-5.7
C_{13}	19.1	15.2	20.4	18.5	-3.1
C_{14}	-18.0	-17.6	2.2	-14.4	20.0

Table 3: Elastic constants for α -quartz calculated at 0 K for different force fields, the experimental results are given for the room temperature ($T = 298$ K).

- [13] WOODCOCK L.V., ANGELL C.A. and CHEESEMAN P., *J. Chem. Phys.*, **65** (1976) 1565
- [14] TSUNYUKI S., TSUKADA M., AOKI H. and MATSUI Y., *Phys. Rev. Lett.*, **61** (1988) 869
- [15] VASHISHTA P., KALIA R.K., RINO J.P. and EBBSJÖ I., *Phys. Rev. B*, **41** (1990) 12197
- [16] WILSON M. and MADDEN P.A., *J. Phys.: Condens. Matter*, **5** (1993) 2687
- [17] WILSON M., MADDEN P.A., HEMMATI M. and ANGELL C.A., *Phys. Rev. Lett.*, **77** (1996) 4023
- [18] JACKSON R.A. and CATLOW C.R.A., *Mol. Simul.*, **1** (1998) 207
- [19] VOLLMAYR K., KOB W. and BINDER K., *Phys. Rev. B*, **54** (1996) 15808
- [20] HORBACH J. and KOB W., *Phys. Rev. B*, **60** (1999) 3169
- [21] HORBACH J., KOB W. and BINDER K., *J. Phys. Chem. B*, **103** (1999) 4104.
- [22] HERZBACH D., BINDER K. and MÜSER M.H., *J. Chem. Phys.*, **123** (2005) 124711
- [23] CPMD, *Copyright IBM Corp 1990-2006, Copyright MPI für Festkörperforschung Stuttgart 1997-2001* (version 3.9.2)
- [24] MAZURIN O.V., STRELTSINA M.V. and SHVAIKO-SHVAIKOVSKAYA T.P., *Handbook of Glass Data, Part A: Silica Glass and Binary Silicate Glasses* (Elsevier, Amsterdam) 1983
- [25] KOHN W. and SHAM L., *Phys. Rev.*, **140** (1965) A1133
- [26] BACHELET G.B., HAMAN D.R. and SCHLÜTER M., *Phys. Rev. B*, **26** (1982) 4199
- [27] TROUILLER N. and MARTINS J.L., *Phys. Rev. B*, **43** (1991) 1993
- [28] MARTYNA G.J., TUCKERMAN M.E. and KLEIN M.L., *J. Chem. Phys.*, **97** (1992) 2635
- [29] MARTYNA G.J., TUCKERMAN M.E., TOBIAS D.J. and KLEIN M.L., *Mol. Phys.*, **87** (1996) 1117
- [30] TUCKERMAN M.E. and PARRINELLO M., *J. Chem. Phys.*, **101** (1994) 1302
- [31] BINDER K. and KOB W., *Glassy Materials and Disordered Solids: An Introduction to Their Statistical Mechanics* (World Scientific, Singapore) 2005
- [32] ALLEN M. and TILDESLEY D., *Computer Simulation of Liquids* (Oxford University Press, Oxford) 1987
- [33] CARRÉ A., BERTHIER L., HORBACH J., ISPAS S. and KOB W., *J. Chem. Phys.*, **127** (2007) 114512
- [34] PRESS W.H., TEUKOLSKY S.A., VETTERLING W.T. and FLANNERY B.P., *Numerical Recipes* (Cambridge University Press, Cambridge) 1992
- [35] BRÜCKNER R., *J. Non-Cryst. Solids*, **5** (1970) 123
- [36] MOZZI R.L. and WARREN B.E., *J. Appl. Cryst.*, **2** (1969) 164
- [37] MAURI F., PASQUARELLO A., PFROMMER B.G., YOON Y.-G. and LOUIE S.G., *Phys. Rev. B*, **62** (2000) R4786
- [38] PETTIFER R.F., DUPREE R., FARNAN I. and STERNBERG U., *J. Non-Cryst. Solids*, **106** (1988) 408
- [39] MIKKELSEN J.C., *Appl. Phys. Lett.*, **45** (1984) 1187.
- [40] BRÉBEC G., SEGUIN R., SELLA C., BEVENOT J. and MARTIN J.C., *Acta Metall.*, **28** (1980) 327.
- [41] GALE J.D. and ROHL A.L., *Mol. Sim.*, **29** (2003) 291
- [42] WILL G., BELLOTTO M., PARRISH W. and HART M., *J. Appl. Cryst.*, **21** (1988) 182
- [43] MCSKIMIN H.J., ANDREATCH P. and THURSTON R.N., *J. Appl. Phys.*, **36** (1965) 1624
- [44] LEVIEN L., PREWITT C.T. and WEIDNER D.J., *Am. Mineral.*, **65** (1980) 920